Dose-Response: An International Journal

Volume 8 | Issue 4 Article 5

12-2010

STOCHASTIC THRESHOLD MICRODOSE MODEL FOR CELL KILLING BY INSOLUBLE METALLIC NANOMATERIAL PARTICLES

Bobby R Scott
Lovelace Respiratory Research Institute, Albuquerque, NM

Dose-Response, 8:428–447, 2010
Formerly Nonlinearity in Biology, Toxicology, and Medicine

ISSN: 1559-3258
DOI: 10.2203/dose-response.09-061.Scott

International Dose-Response Society
www.Dose-Response.org

STOCHASTIC THRESHOLD MICRODOSE MODEL FOR CELL KILLING BY INSOLUBLE METALLIC NANOMATERIAL PARTICLES

Bobby R. Scott □ Lovelace Respiratory Research Institute

□ This paper introduces a novel microdosimetric model for **me**tallic **na**nomaterial-**p**articles (MENAP)-induced cytotoxicity. The focus is on the engineered insoluble MENAP which represent a significant breakthrough in the design and development of new products for consumers, industry, and medicine. Increased production is rapidly occurring and may cause currently unrecognized health effects (e.g., nervous system dysfunction, heart disease, cancer); thus, dose-response models for MENAP-induced biological effects are needed to facilitate health risk assessment. The ***s**tochastic **t**hreshold **m**icrodose (STM) model* presented introduces novel stochastic microdose metrics for use in constructing dose-response relationships for the frequency of specific cellular (e.g., cell killing, mutations, neoplastic transformation) or subcellular (e.g., mitochondria dysfunction) effects. A key metric is the exposure-time-dependent, *specific burden* (MENAP count) for a given critical target (e.g., mitochondria, nucleus). Exceeding a stochastic threshold specific burden triggers cell death. For critical targets in the cytoplasm, the autophagic mode of death is triggered. For the nuclear target, the apoptotic mode of death is triggered. Overall cell survival is evaluated for the indicated competing modes of death when both apply. The STM model can be applied to cytotoxicity data using Bayesian methods implemented via Markov chain Monte Carlo.

Keywords: microdosimetric model, nanomaterials, cytotoxicity

INTRODUCTION

Billions of dollars have recently been invested worldwide in nanotechnology research and development (Roco 2005). This is because nanomaterials have properties that make them useful for many applications, including high conductivity, material strengthening, increasing material durability, and altering material reactivity. Numerous nanomaterials are made of metals or metal oxides. The metals include iron, gold, zinc, silver, copper, lead, cerium, zirconium, cadmium, germanium, and selenium. Important **e**ngineered **n**ano**m**aterial (ENM) now in production include metal oxides, fullerenes, carbon nanotubes, and quantum dots. A variety of bionanotechnologies are also being developed for biomedical applications. For example, ENM particles are being researched for possible use in cancer therapy (AshaRani *et al.* 2009); however, not very much is known about health risks to nanotechnology workers and the general public for ENM particles (Donaldson *et al.* 2004; Moghimi *et*

Address correspondence to Bobby R. Scott, Lovelace Respiratory Research Institute, 2425 Ridgecrest Drive SE, Albuquerque, NM 87108; E-mail: bscott@LRRI.org

al. 2005; Oberdörster *et al.* 2005; Hardman 2006; Powell and Kanarek 2006a,b; Prabhu *et al.* 2009).

ENM particles are typically defined as engineered particles having at least one dimension <100 nanometers (nm). The particles could be inhaled, ingested, or enter the body via uptake through the skin (intact or wounded).

Because of their small size, ENM particles have distinct properties compared with the bulk form of the same materials. When inhaled, ENM particles are efficiently deposited by diffusion-related mechanisms in all regions of the respiratory tract. Their small size facilitates uptake into cells and *transcytosis* across epithelial and endothelial cells into the blood and lymph circulation to potentially reach targets such as bone marrow, lymph nodes, spleen, and heart (Oberdörster *et al.* 2005). Translocation to the nervous system via axons and dendrites of neurons has also been observed (Oberdörster *et al.* 2005). In addition, mitochondria have been identified as a key cytoplasmic target for uptake of ENM particles (Oberdörster *et al.* 2005).

In a biological fluid, proteins associate with ENM particles, and the amount and presentation of the proteins on the surface of the particles can influence biological responses. Proteins compete for the nanoparticle surface, leading to a *protein corona* that largely defines the biological identity of the particle. Thus, knowledge of rates, affinities, and stoichiometries of protein association with, and dissociation from, nanoparticles is important for understanding the nature of the particle surface seen by the functional machinery of cells.

Potential biological effects of ENM particles include DNA damage, mitochondrial damage, mutations, cell killing and related systemic effects (inflammation, cancer, thrombosis, nervous system dysfunction, fibrosis and heart disease) (Powell and Kanarek 2006a,b; AshaRani *et al.* 2009). *Mitochondrial damage to cells in cardiac tissue is a suspected contributor to heart disease.*

The focus of the modeling in this paper is on insoluble engineered **me**tallic **na**nomaterial **p**articles (MENAP). *In vitro* studies using normal human fibroblast have demonstrated that the cellular uptake of insoluble engineered MENAP (silver nanoparticles) occurred mainly through endocytosis (clathrin-mediated process and macropinocytosis), accompanied by what was interpreted as a time-dependent increase in the exocytosis rate (AshaRani *et al.* 2009). The authors however did not control for the release of particles when cell killing occurs which may be the major source of the particle concentration increases in the cell culture media over time. Electron micrographs revealed that the MENAP were uniformly distributed in both the cytoplasm and nucleus (AshaRani *et al.* 2009). Thus, biological targets in both the cytoplasm and nucleus can be at risk for being damaged by insoluble MENAP. Should it be proven (by

new research) that the increases in time of MENAP in cell culture media mainly relate to cell killing, then such an increase could be used as a biomarker for cell killing *in vitro*.

The purpose of this paper is to introduce a novel mathematical model for application to characterizing the cell killing effects of insoluble engineered MENAP. Unlike deterministic models which have been applied to soluble macroscopic size particles, stochastic models are needed for characterizing biological effects of insoluble MENAP exposure of cells in the body or in cell culture, especially for low and moderate levels of exposure as might be expected for the general public. This paper introduces a novel *microdosimetric model*. To date, microdosimetric modeling of stochastic biological effects on cells has mainly been in the field of radiation research. Here, a similar approach as has been used for radiation-induced cytotoxicity is used for characterizing MENAP cytotoxicity. The focus is on cell killing via one of two potentially competing modes (apoptotic and autophagic) of programmed cell death. Different dose metrics are proposed for the two modes of death.

Programmed cell death comprises two subtypes, as have been discovered using electron microscopy. Apoptosis (type-I programmed cell death) is characterized by condensation of the cytoplasm and preservation of organelles, essentially without autophagic degradation (Bursch *et al.* 2000). On the other hand, autophagic cell death (type-II programmed cell death) exhibits extensive autophagic degradation of Golgi apparatus, polyribosomes and endoplasmic reticulum, which precedes nuclear destruction (Bursch *et al.* 2000). It is presumed here that apoptosis is triggered by nuclear DNA damage sensing pathways while autophagic cell death is triggered by damage occurring in unspecified cytoplasmic targets (suspected to be mitochondria).

Because MENAP can enter and persist in the cytoplasm or translocate to the nucleus and persist there, a microdosimetric approach should be considered when modeling both *in vitro* and *in vivo* stochastic biological effects of these particles. This includes effects such as mitochondria dysfunction, endoplasmic reticulum dysfunction, mutation induction, neoplastic transformation, cell killing, and cancer induction. Cytoplasmic organelle dysfunction could be a contributing factor for later occurring diseases such as cardiovascular diseases. The MENAP induced cytotoxicity could also lead to debilitating diseases such as pulmonary fibrosis. This however needs to be researched.

The model presented here does not address the transport of MENAP to the site of the target cells or the kinetics of particle uptake by these cells. *These modeling components must be provided by other research efforts.* The focus here is on a hypothetical buildup over time of MENAP in a hypothetical target-cell population and the cytotoxic consequences. The target population is treated here as a homogenous cell population as occur in

many cell culture studies (e.g., macrophages, bronchial epithelial cells, fibroblast, etc.). In fact the model presented can be most easily applied to cell culture studies of MENAP cytotoxicity. A more involved approach will apply to *in vivo exposures* because one will need to address the particokinetics that lead to the transport and uptake of MENAP by the target cell population, the macroscopic and microscopic biodistributions of particles of interest and the biological response of a heterogeneous target-cell population.

STOCHASTIC THRESHOLD MICRODOSE MODEL FOR CELL KILLING

The **S**tochastic **T**hreshold **M**icrodose (STM) model introduced in this section allows evaluation of the fraction of a target cell population without lethal damage (survival fraction) after MENAP exposure of a given homogeneous target cell population for a period of time t. The model applies to insoluble MENAP. Thus, particle dissolution and subsequent metabolism is not relevant; however, the model allows for surface characteristics of MENAP being modified by the biological media that surrounds them (e.g., corona formation). The STM model is based on the individual cell *specific burden* (particle count) $B(t)$ for a given critical target (e.g., nucleus), which is assumed to have a Poisson distribution. The burden $B(t)$ is the number of MENAP contained within a specified individual target (e.g., nucleus) at exposure time t and depends on MENAP dynamics (e.g., rate of uptake). When the entire cytoplasm is considered a critical target, the burden of interest is the *specific cytoplasmic burden* $B_c(t)$ with the subscript c representing "cytoplasm". When the nucleus is considered a critical target, the burden of interest is the *specific nuclear burden* $B_n(t)$, with the subscript n representing "nucleus". When mitochondria in the cytoplasm are considered the critical target, the burden of interest is the specific mitochondrion burden $B_m(t)$, with the subscript m representing "mitochondria". Thus, $B_m(t)$ is evaluated over different mitochondria in a given cell as well as mitochondria in other target cells. In contrast, $B_n(t)$ is evaluated over the different target cells, since there is a single nucleus per cell. The indicated specific burdens are stochastic (i.e., random variables governed by the laws of probability) and exposure-time-dependent. Thus, $B_m(t)$ varies for different mitochondria and $B_n(t)$ varies for different nuclei and both have presumed Poisson distributions as previously indicated. Variation in the specific burden is expected to contribute to variability in biological response to MENAP.

The indicated three dose metrics can be represented by the covariate vector $\mathbf{B}(t) = (B_c(t), B_n(t), B_m(t))$ of specific burdens, which can be used in dose-response modeling. The expectation (average) values of $B_c(t)$, $B_n(t)$, and $B_m(t)$ are also useful deterministic dose metrics and are respectively represented by what are formally called the *cytoplasmic burden* $M_c(t)$,

nuclear burden $M_n(t)$, and *mitochondria burden* $M_m(t)$. The averaging applies to a given value for the exposure time t; thus, averaging is not done over different follow-up times. Ideally, the indicated averages would be evaluated based on imaging data (e.g., using fluorescent MENAP) after exposure for time t; however, the resources to achieve this may not be readily available. In such cases, the indicated burdens (distributions and related averages) can be estimated from dose-response data by fitting the STM model to the data using a Bayesian approach implemented with Markov chain Monte Carlo. This will be demonstrated in a follow-on paper to be submitted to this journal.

The indicated averages can also be represented by a corvariate vector, $\mathbf{M}(t) = (M_c(t), M_n(t), M_m(t))$, of particle burdens, which can be used in dose-response modeling. It is assumed that $\mathbf{M}(t)$ (i.e., $M_c(t)$, $M_n(t)$, and $M_m(t)$) increases monotonically for a period of time because of particle uptake and decrease thereafter because of cells with large MENAP burdens being killed leaving a surviving cell population with lower particle burdens as were reported by AshaRani *et al.* (2009) in their in vitro studies. For the presumed delayed cell killing phase, the concentration of particles in the extracellular spaces in vivo or in cell culture media is assumed to mainly increase due to particle releases from dying cells rather than via exocytosis as may have been incorrectly assumed by AshaRani *et al.* (2009).

With the stochastic cell killing model introduced here, accumulating a specific cytoplasmic target burden that exceeds a threshold value N_j for target j (e.g., $j = m$ for mitochondria) triggers the autophagic pathway to death. Similarly, a specific nuclear burden $B_n(t)$ that exceeds a threshold N_n triggers the apoptotic pathway to cell death when the autophagic path has not already been triggered. Further, both N_j and N_n are assumed to be stochastic (i.e., differs for different cells) and to depend on the type of MENAP and their influential characteristics. This allows for influences on N_j and N_n of the interactions of MENAP with biological materials in the body and in cell culture. It also allows for the varying potency (i.e., ability to produce biological damage) of the different types of MENAP. The potency in turn allows for evaluation of relative potency. The expectation values for N_j and N_n are given by μ_j^* and μ_n^*, respectively. MENAP potency for the autophagic mode of cell death is then evaluated as $1/\mu_j^*$; for the apoptotic mode it is evaluated as $1/\mu_n^*$. Thus, for mitochondria as the critical cytoplasmic target for MEMAP cell killing, potency is given by $1/\mu_m^*$.

The notion of stochastic thresholds for biological effects in cells was introduced by this author in an earlier paper (Scott 2005) that relates to radiation-induced biological effects (apoptosis and neoplastic transformation). The existence of a stochastic threshold adds to the variability in the biological response to MENAP exposure. The added variability is beyond what can be attributed to variability in the microdose to the critical biological target. Thus, stochastic models are needed to address such

variability. For this reason conventional toxicology models (which are deterministic) that are based on macroscopic dose metrics (e.g., MENAP concentration) may fail when attempting to account for variability in biological responses to MENAP. The variability could be rather large. In addition, the STM model allows predicting cytotoxicity for any assigned Poisson distribution of MENAP hits (uptakes) to the critical biological target (e.g., mitochondria) for a given value of the particle potency. This is not possible with conventional models.

Imaging for counting MENAP burden distributions over live cells would allow for evaluating $M_j(t)$ and $M_n(t)$ for different exposure times when the critical cytoplasmic target has been identified. The imaging would also allow for determining whether the specific burdens of interest have Poisson distributions; however, *new research is needed to achieve this and to develop particokinetic models for evaluating* $M_j(t)$ *and* $M_n(t)$ for different exposure times. With particokinetic models for evaluating $M_j(t)$ and $M_n(t)$ and experimental data for the proportion of cells that are killed via autophagic and apoptotic pathways, the distribution $\Phi_j(N_j)$ of N_j and distribution $\Phi_n(N_n)$ of N_n could be estimated (as a hidden Markov model [HMM] (Rabiner 1989)) from dose-response data for cell survival using Bayesian methods implemented using Markov chain Monte Carlo (Gamerman 1997; Gelman *et al.* 1995). With Poisson distributions for the specific burdens and threshold number of particles for causing lethality, the respective means μ_j and μ_n of the distributions could be estimated as free parameters when fitting the STM model to data.

To facilitate data analysis when both the autophagic and apoptotic modes of death operate as competing risks, the cytotoxicity data can be adjusted to remove a competing mode of death (e.g., eliminating the apoptotic mode to focus on the autophagic mode). This would reduce the number of model parameters that need to be estimated for a given analysis. The hypothetical examples presented here relate to such data.

Here an empirical function is used to estimate $M_j(t)$ and $\Phi_j(N_j)$ is assumed to represent a Poisson distribution with mean μ_j, which depends on the physical, chemical, and other characteristics of the MENAP and target cell population..

The cytoplasmic target burden $M_j(t)$ is estimated here using the monotonically increasing function $\Phi(t|T_{1/2}, C_{\max}\{V\})$, where:

$$\Phi(t|\ T_{1/2}, C_{\max}\{V\}) = C_{\max}\{V\}\{1 - \exp(-[\ln(2)]\, t/T_{1/2})\}. \qquad (1)$$

The deterministic parameter $C_{\max}\{V\}$ is the expectation value for maximum number of particles that enter and remain in the target of interest (cytoplasmic target) of the at-risk cell population and can be estimated from data from cell imaging experimental studies (e.g., *in vitro* studies) that focus on evaluating $M_j(t)$ for different follow-up times for a

given target cell population. The deterministic variable V is the average target (cytoplasmic target or nucleus) volume. The deterministic variable $T_{1/2}$ is the half-time for target cells being MENAP-free for the period over which particle uptake progressively increases. Equation 1 can be justified if particles from a modest size pool behave such that the number of particles, X, available for uptake decreases with exposure time t according to the equation, $dX/dt = A - kX$, where A and k are constants. Equation 1 therefore applies to the exposure time period prior to the time point at which significant cell killing occurs. At the indicated time point, subtle changes in $M_j(t)$ could occur (e.g., due to loss of cells with large burdens). An estimate of $M_j(t)$ is $\Phi(t|T_{1/2}, C_{\max}\{V_j\})$, where V_j is the cytoplasmic target volume averaged over the target cell population. Similarly, an estimate of $M_n(t)$ is $\Phi(t|T_{1/2}, C_{\max}\{V_n\})$, where V_n is corresponding average nuclear volume.

In circumstances where one has a fixed exposure time but different levels of exposure to MENAP, one can also estimate $M_j(t)$ and $M_n(t)$ for the indicated exposure time based on a **d**ose **c**onversion **f**actor (DCF) which is treated as a free parameter. For example, when only the autophagic mode of death applies (e.g., data adjusted to remove apoptotic deaths or only this mode occurs), and the exposure concentration, C, exposure time (t=T) product (CT) is known, then $M_j(t) = DCF_j * CT$ can be used when fitting the STM model to real data, with DCF_j as a free parameter to be estimated for critical target j. Bayesian inference methods implemented with Markov chain Monte Carlo allow for such evaluations as will be demonstrated in a subsequent paper that applies the STM model to real data.

RESULTS

Simulations were conducted for a hypothetical *in vitro* study where insoluble MENAP are injected into cell cultures and cell killing via apoptosis and autophagy was carefully monitored over time after injection. The MENAP considered were monodisperse spherical particles with an average diameter of 1 nm. Cytoplasmic particles were considered to be filtered by mitochondria, reducing the number available for uptake by the nucleus. The autophagic mode of death for this example was triggered when the specific mitochondrion burden exceeded a Poisson distributed value N_m with expectation value $\mu_m = 5$. It was assumed that the cell killing data were adjusted to eliminate the effect of the apoptotic pathway deaths. The parameter $C_{\max}\{V_m\}$ was assigned the arbitrary value of 10 MENAP on average. The parameter $T_{1/2}$ was assigned the arbitrary value of 20 minutes. These values were used for illustrative purposes and are not based on having evaluated any real data. Figure 1 shows the pattern of change for $M_m(t)$ when calculations were carried out for 0, 1, 2, 4, 8,

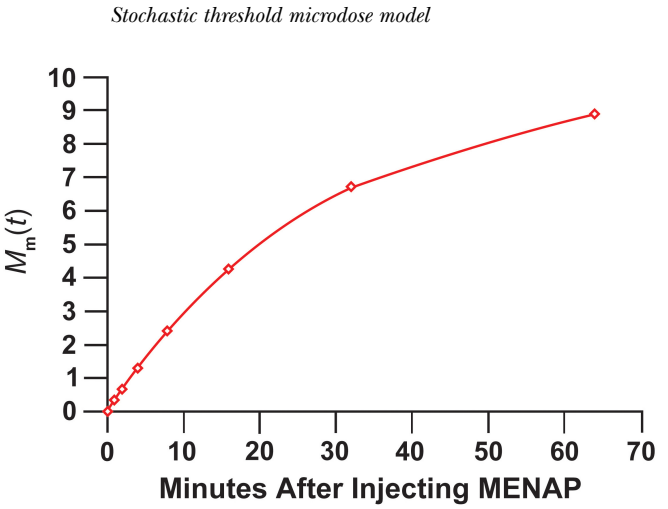

FIGURE 1. Hypothetical pattern for the mitochondria burden, $M_m(t)$, for a MENAP exposure scenario where Equation 1 applies and $C_{max}\{V_c\} = 10$ and $T_{1/2} = 20$ minutes.

16, 32, and 64 minutes after MENAP injection. The smooth curve was obtained using Excel smoothing software to connect the calculated points. Adding more time points may alter the curve shape somewhat. This is why the data points were also plotted as they will not change with additional time points being included.

Crystal Ball (Decisioneering 2001) software was used to implement the STM model. The assignment of $\mu_m = 5$ means that on average 5 MENAP per mitochondrion would have to be exceeded for triggering autophagic-mode lethality. A smaller value for μ_m may be more realistic, depending on the susceptibility of the target cell population; however. Figure 2 shows the simulated MENAP distributions for mitochondria for follow-up times of 1, 2, 4, 8, 16, 32, and 64 minutes. These times are indicated by T1, T2, T4,…, respectively; however, not all times could be labeled in the figure due to cluttering so that labels for some times points are not indicated as explained in the figure legend. Figure 3 shows the calculated fraction (hypothetical) of target cells that did not receive lethal mitochondrial damage (triggered by more than N_m MENAP) for different follow-up times. Results apply to circumstances where only the autophagic mode of cell death occurs (e.g., where data are adjusted to eliminate the apoptotic mode). Figure 4 shows the corresponding dose-response relationship when the mitochondria burden $M_m(t)$ is used as the dose metric. Results are based on 100,000 Monte Carlo realizations for the survival fraction which were evaluated using the Excel Poisson distribution cumulative probability function for N_m events (stochastic) when the mean is $M_m(t)$. The data points in the central curve are averages over the 100,000 values generated. Excel smoothing functions were used for connecting the data points in the figure. The upper curves in Figures 3

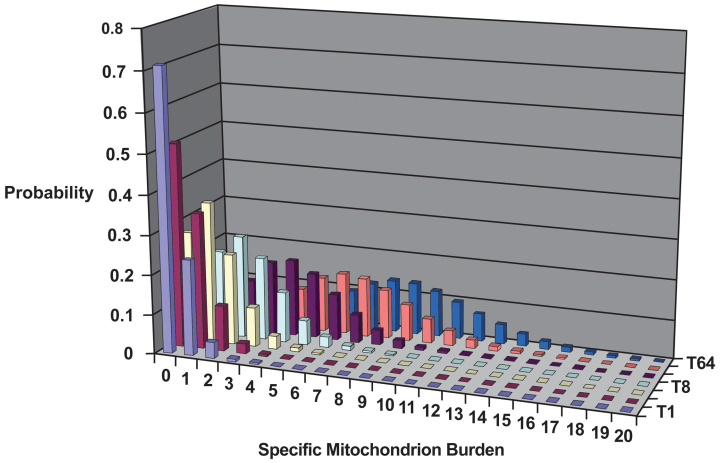

FIGURE 2. Simulated cell MENAP microdose distribution (particles per mitochondrion) vs. follow-up time after the insoluble monodisperse spherical particles are injected into cell culture. Average burdens are evaluated based Equation 1 with $C_{max}\{V_c\}$=10 and $T_{1/2}$ = 20 min. From the front to back rows, follow-up times are 1 minute (T1), 2 min, 4 min, 8 min (T8), 16 min, 32 min, and 64 min (T64).

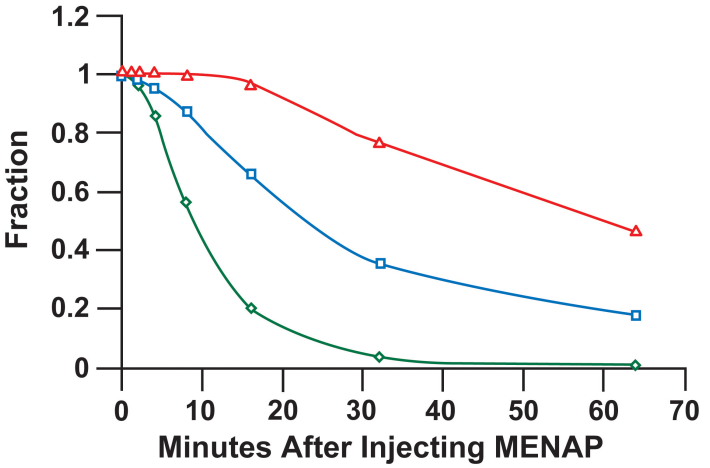

FIGURE 3. Simulated fraction of cells without lethal damage after exposure to insoluble MENAP particles in cell culture based on the STM model. The results apply to a data set for which only the autophagic mode of cell death occurs (e.g., data or adjusted to eliminate the apoptotic mode deaths). Data points on the central curve are the average of 100,000 Monte Carlo realizations. The 90th (upper curve) and 10th (lower curve) percentiles results are also presented. Model parameter assignments are provided in the main text.

and 4 represent the 90th percentile of the distribution and the lower curves represent the 10th percentile. These percentiles were arbitrarily selected from the set of percentiles provided in Crystal Ball output. The wide variability in Figure 4 relates to extra Poisson variability beyond what can be explained based on the Poisson distribution of MENAP uptake (hits) by mitochondria. The extra variability relates to the stochastic

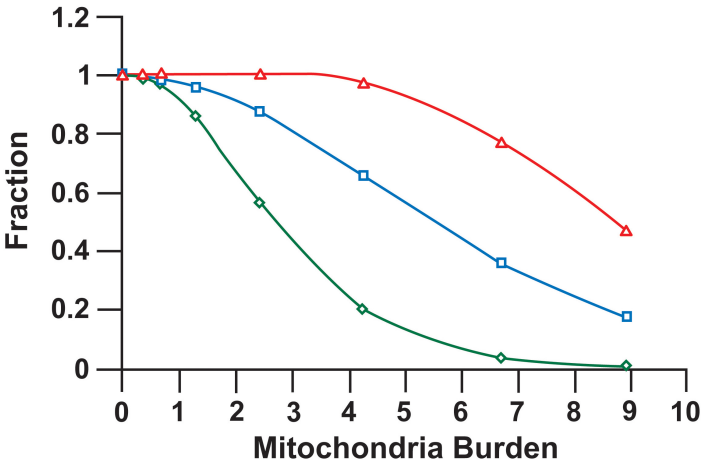

FIGURE 4. Same data as in Figure 3 but plotted as a function of the mitochondria burden of MENAP.

threshold N_m for triggering the autophagic mode of cell death. The variability in the survival fraction presented in Figure 4 for $M_m(t) = 1$ is consistent with data reported by Prabhu *et al.* (2009) for the in vitro cytotoxicity of 80 nm copper nanoparticles to somatosensory neurons.

Similar results as in Figures 3 and 4 can be obtained when cell killing via apoptosis is the focus and the biological data are adjusted to correct for the autophagic mode of death; however, $M_n(t)$ is expected to depend on mean MENAP transport time, τ, through the cytoplasm to the nucleus. Figure 5 shows a hypothetical nuclear MENAP distribution based on $C_{\max}\{V_n\} = 4$ and $T_{1/2}$ still at 20 min. Assuming independence of the two modes of death, one can then generate cell survival curves (population averages) for both competing modes of death using the STM model as illustrated in Figure 6.

DISCUSSION AND CONCLUSIONS

Results in Figure 6 are based on the MENAP mitochondrial and nuclear distributions in figures 2 and 5 and N_m having a Poisson distribution with mean $\mu_m = 5$ and N_n having a Poisson distribution with mean $\mu_n = 1$. The upper curve is for the apoptotic mode of death (when autophagy is eliminated); the middle curve is for the autophagic mode of death (when apoptosis is eliminated), and the lower curve is when both modes of cell death apply. For independent modes of death, the respective survival fractions multiply (rather than add; a result of probability theory). Also, the bottom curve was not obtained by multiplying the middle and top curves (which are population averages) but rater represents averaging over 100,000 results (generated from data points on many different middle and upper curves).

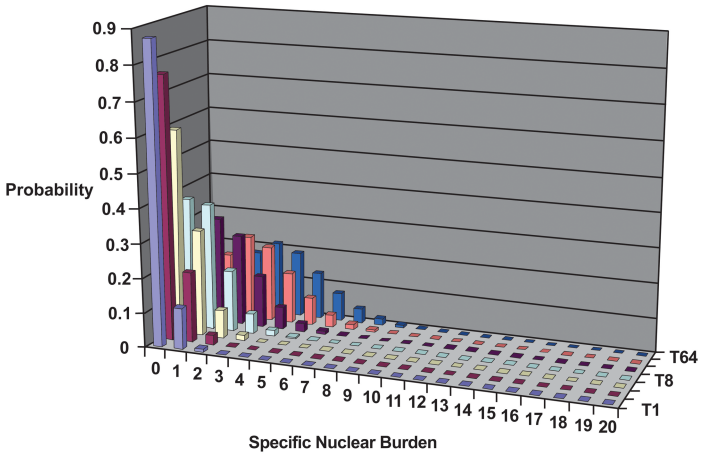

FIGURE 5. Simulated cell MENAP microdose distribution (nuclear particles per cell) vs. follow-up time after the particles are injected into cell culture. Average nuclear burdens are evaluated based on Equation 1 with $C_{\max}\{V_n\}$=4 and $T_{1/2}$ = 20 min. From the front to back rows, follow-up times are 1 minute (T1), 2 min, 4 min, 8 min (T8), 16 min, 32 min, and 64 min (T64).

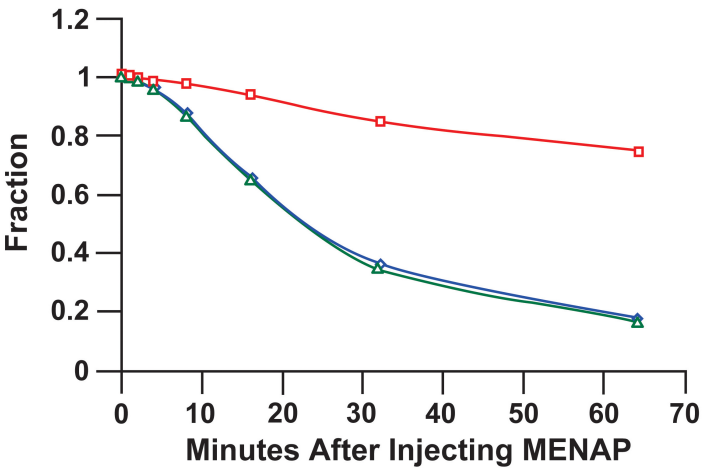

FIGURE 6. Simulated expected fraction of cells without lethal damage after exposure to MENAP particles in cell culture based on the STM model and the microdose distributions in Figures 2 and 5. The upper curve relates to the apoptotic deaths due to nuclear damage when data are corrected to eliminate autophagic-mode effects. The middle curve is the corresponding curve for deaths via the autophagic mode (corrected for apoptotic-mode effects). The bottom cure allows for both modes of death. Each of the data points on the three curves are averages of 100,000 Monte Carlo realizations.

Results similar to those presented in Figure 6 can be generated with specific experiments that focus on application of the proposed model. *It will be important to design the studies in a way that allows evaluation of the appropriate particokinetics model to use for describing $M_j(t)$ and $M_n(t)$ for the period of time over which particle intake by cells increases monotonically.* It is reasonable

to expect that $M_j(t)$ and $M_n(t)$ will be found to indeed depend on $C_{\max}(V)$ (as implicated by Equation 1) and that $M_n(t)$ will be found to depend on τ, which may in turn be influenced by MENAP particle biological coronas.

With $M_j(t)$ and $M_n(t)$ known (i.e., estimated) and experimental data available for the proportion of the target cells that are killed via apoptosis and via autophagy over different follow-up times, Bayesian methods (Gelman *et al.* 1995; Gamerman 1997) could then be employed to determine the functional form that best represents the distribution of N_j and N_n. Should these distribution be very narrow, this would implicate fixed values for N_j and N_n. It is anticipated that the functional form for $M_j(t)$ and $M_n(t)$ and the distributions of N_j and N_n (or a fixed value for them) may depend on physical and other characteristic of the MENAP and may also depend on interactions of the MENAP with the cellular/tissue environment studied (e.g., corona formation). Irrespective of the form of the distributions $\Phi_j(N_j)$ and $\Phi_n(N_n)$, their true means (here indicated μ_j^* and μ_n^*, respectively) can be used for characterizing relative potency (*RP*) for two different types of MENAP using the following relationship:

$$RP = \mu_k^*\{\text{type-R particles}\}/\mu_k^*\{\text{type-T particles}\}. \quad (2)$$

Here type-T refers to a *test* MENAP type and type-R refers to a *reference* MENAP type and k takes on the value j for the autophagic and n for the apoptotic modes of death, respectively.

For Poisson distributions for N_j and N_n, $\mu_j^* = \mu_j$ and $\mu_n^* = \mu_n$. It is possible that *RP* estimates for cytotoxicity developed using the STM model and *in vitro* data may also apply to *in vivo* effects that are a consequence of cell killing for the target cell population of interest. *This needs to be investigated.*

It is expected that similar *RP* relationships can be developed based on applying microdosimetric models to other endpoints such as mutations, neoplastic transformation, mitochondria dysfunction, *etc.*; further, these *RP* values may be predictive of *RP* for *in vivo* effects such as cancer and heart disease. However, *these cross-scale extrapolations will need to be investigated through a focused research program.*

Experimentally-derived cell survival fractions for the autophagic, $S_j(t)$, and apoptotic, $S_n(t)$, modes (i.e., adjusted to eliminate the competing mode) can be fitted using the STM model. The fitted lethality-mode-specific survival values can then be used to obtain corresponding hazard functions $H_j(t)$ and $H_n(t)$ (which are continuous cumulative hazard functions) that could possibly be used to link cellular damage to tissue level risks (e.g., pulmonary fibrosis, heart disease). For example, the tissue level effect (e.g., fibrosis) hazard function could possibly be evaluated as a function of $H_j(t)$ or $H_n(t)$ or $H_j(t)+H_n(t)$.

TABLE 1. Plausible dose and dose rate metrics for characterizing cellular and intracellular effects of insoluble MENAP in cell cultures

Biological Target	Dose Metric	Dose Rate Metrica
Cell surface	MENAP average concentration in culture media multiplied by time the target cells are at risk	MENAP average concentration in culture media
Cytoplasmic target (e.g., mitochondria)	$B_j(t)$, $M_j(t)$	$b_j(t)$, $m_j(t)$
Nucleus	$B_n(t)$, $M_n(t)$	$b_n(t)$, $m_n(t)$

[a]$b_j(t) = d(B_j(t))/dt$; $m_j(t) = d(M_j(t))/dt$; $b_n(t) = d(B_n(t))/dt$; $m_n(t) = d(M_n(t))/dt$. The metrics $B_j(t)$ and $B_n(t)$ relate to individual targets. The metrics $M_j(t)$ and $M_n(t)$ are averaged over the target cell population and can be estimated as HMM (Hidden Markov Models) using Bayesian inference methods. The distributions of $B_j(t)$ and $B_n(t)$ can be presumed to be Poisson distributions with expectation values $M_j(t)$ and $M_n(t)$, respectively, unless data indicate otherwise.

The hazard functions $H_j(t)$ and H_n(t) are formally called *cell lethality hazards* as they relate to induced cytotoxicity. Reactive oxygen and nitrogen species may play a key role in evolution of the cell lethality hazards as has been found for radiation exposure. The linking of cellular damage to tissue-level risks will be addressed in subsequent research.

The indicated cell lethality hazards are evaluated as follows:

$$H_j(t) = -\ln[S_j(t)] \tag{3}$$

$$H_n(t) = -\ln[S_n(t)]. \tag{4}$$

The overall cell survival fraction, $S(t)$, can also be evaluated using the total cell lethality hazard $H(t)$ (which is the sum of $H_c(t)$ and $H_n(t)$) as follows:

$$S(t) = \exp[-H(t)]. \tag{5}$$

Table 1 presents plausible dose and dose-rate metrics for characterizing cellular and intracellular effects (physical stress responses) of exposure of cell cultures to insoluble MENAP. For effects that relate to particle interactions with cell surface receptors, a plausible dose metric is the product of the average MENAP concentration in the culture media multiplied by the time the cells are at risk of being damaged (here called exposure time). The exposure time is considered important because the number of MENAP interactions with cell surface receptors is expected to increase over time. The derivative of the metric with respect to time gives a plausible dose rate metric, namely the MENAP concentration in culture media. *These metrics could also be applied to characterizing biological effects of*

MENAP transported in the systemic circulation in the body that result from interactions with blood cell surface receptors.

For developing dose-response relationships for biological effects that relate to cytoplasmic organelle damage, M_j(t) (e.g., $M_m(t)$ for mitochondria damage) is a plausible dose metric (irrespective of the relevance of Equation 1). In addition, the derivative with respect to exposure time, $m_j(t) = d(M_j(t))/dt$, is a plausible dose-rate metric for these effects. The metric $m_j(t)$ is formally called the *cytoplasmic target hit rate*. For cases where mitochondria are the critical target, then $m_m(t)$ would represent the *mitochondria hit rate*.

For developing dose-response relationships for biological effects that relate to damage to targets in the nucleus (e.g., DNA, histones), $M_n(t)$ is a plausible dose metric (irrespective of the relevance of Equation 1). In addition, the derivative with respect to time, $m_n(t) = d(M_n(t))/dt$, is a plausible dose-rate metric for these effects. The metric $m_n(t)$ is formally called the *nuclear hit rate*.

It follows that $M_n(t)$ and $m_n(t)$ could be used when developing dose-response relationships for the frequency DNA single-strand breaks, DNA double-strand breaks, chromosomal aberrations frequency, micronuclei induction frequency, apoptosis frequency, mutation induction frequency, and neoplastic transformation frequency. For *in vivo* studies, these variables could also be used for developing dose-response relationships for cancer when evaluated for the critical target cell population; however, *particokinetics models will be needed to characterize transport of MENAP to the target cell population (e.g., cardiac tissue), uptake by the target cells, and transport to the cell nucleus*. The nuclear hit rate, $m_n(t)$, is expected to be useful for accounting for dose-rate effects on DNA repair, mutations, neoplastic transformation, and cancer. While only a limited number of dose metrics are used here for MENAP, there are also other plausible dose metrics (some correlated) as discussed below.

The focus of the modeling approach presented here was on induced cell lethality via autophagy or apoptosis. A similar competing-risk approach can be used to include MENAP-induced mutations, neoplastic transformation (formation of precancerous cells), or mitochondria dysfunction. For endpoint such as mutations and neoplastic transformation *in vitro*, low-level exposure to MENAP may stimulate an adaptive response (protection against harm) whereby there is a decrease rather than an increase in the stochastic biological effect of interest (Scott 2005). Such effects are called *protective bystander effects* and may involve epigenetic signaling pathways (Scott *et al.* 2009). Indeed, it is now considered likely that epigenetic silencing of adaptive response genes triggered by high dose exposure to agents such as ionizing radiation and genotoxic chemicals plays a major role in cancer induction (Scott *et al.* 2009). *The STM model presented in this paper does not address protective or deleterious bystander effects.*

For some target cell populations and for a specific type of MENAP, only one mode of cell death may apply (e.g., autophagic mode due to mitochondrial damage). In such cases results presented will still apply; however, information may not be available on the microdosimetric variable of interest (e.g. $M_m(t)$). This limitation can be overcome through use of the dose conversion factor DCF_j. For example when mitochondria is the critical target, then $M_m(t) = DCF_m * CT$ can be evaluated as a HMM (Hidden Markov Model) given observed values of CT and the biological effect of interest. With estimates of $M_m(t)$, one can then generate Poisson distributions for the mitochondrion burden as presented in Figure 2. Use of software such as WinBUGS (Lunn *et al.* 2000) allows carrying out such calculations at the same time as fitting the STM model to real data. This will be demonstrated in a subsequent paper where the STM model is applied to *in vitro* data for the cytotoxicity of MENAP.

This paper has presented a scientific basis for the use of microdosimetric modeling in MENAP toxicity research. For the microdosimetric model presented to be used for *in vivo* applications, particokinetic models are needed to evaluate the transport and time-dependent biodistribution of insoluble MENAP particles in the body (including uptake by cells and transport to the nucleus). Initial modeling can be based on *in vitro* (particle uptake by cells) and animal (particle transport and biodistribution) studies using specific routes of exposure (e.g., inhalation or skin application). MENAP *RP* (based on different MENAP characteristics) for specific stochastic effects (cytotoxicity, mutations, neoplastic transformation, mitochondria dysfunction, etc.) can be established based on *in vitro* studies and possibly applied to *in vivo* exposure scenarios.

The cellular lethality hazard functions $H_j(t)$ and $H_n(t)$ could possibly be used to relate cell damage to tissue damage risk when the tissue damage relates to the level of cell killing (e.g., fibrosis) or cytoplasmic organelle residual damage (e.g., mitochondria dysfunction related heart disease) as already indicated. Proportional hazards $H_j(t)/H_j(0)$ and $H_n(t)/H_n(0)$ can be used for evaluating relative risk for low-level exposures. It is expected that relative risk for some stochastic effects (e.g., neoplastic transformation *in vitro*) may be predictive of relative risk for cancer *in vivo* as has been demonstrated for radiation (Redpath *et al.* 2001).

It will be important to generate quantitative data for the frequency of the specific *in vivo* biological effect of interest (e.g., heart disease, pulmonary fibrosis, lung cancer) as a function of a plausible dose metric (e.g. $M_j(t)$, or $M_n(t)$, or a metric that is correlated with these metrics). *A metric that would be expected to be correlated with $M_j(t)$ and $M_n(t)$ is the time-dependent MENAP concentration in the target tissue (e.g., lung, heart, liver, spleen) integrated up to time t.* Other correlated metrics are discussed below.

Table 2 summarizes formal names, methods of obtaining, and dose-response characterization applications of the dose metrics introduced in

TABLE 2. Formal names, methods of obtaining, and dose-response characterization applications of novel MENAP dose and dose-rate metrics

Dose Metric	Formal Name	Method of Obtaining	Dose-response Characterization Applications
$B_j(t)$	Specific cytoplasmic target burden (for target *j*)	Live cell imaging or Bayesian analysis using MCMC and assuming a Poisson distribution with mean $M_j(t)$	Stochastic effects that relate to damage to cytoplasmic organelles (e.g., mitochondria)
$B_n(t)$	Specific nuclear burden	Live cell imaging or Bayesian analysis using MCMC and assuming a Poisson distribution with mean $M_n(t)$	Stochastic effects that relate to damage to the nuclear contents (e.g., mutations)
$M_j(t)$	Cytoplasmic target burden (for target *j*)	Averaging of measured values for $B_j(t)$ or calculating *via* use of DCF_j when conducting Bayesian analysis	Stochastic and deterministic effects that relate to damage to cytoplasmic organelles
$M_n(t)$	Nuclear burden	Averaging of the measured values for $B_n(t)$ or calculating via use of DCF_n when conducting Bayesian analysis	Stochastic and deterministic effects that relate to damage to nuclear contents (e.g., DNA, histones)
$m_j(t)$	Cytoplasmic target hit rate (for target *j*)	Estimated[1] as $[M_j(t+\Delta t)-M_j(t)]/\Delta t$	Dose rate influence on stochastic effects that relate to cytoplasmic organelles
$m_n(t)$	Nuclear hit rate	Estimated as $[M_n(t+\Delta t)-M_n(t)]/\Delta t$	Dose rate effects that relate to damage to nuclear contents

[1]The variable Δt is a small increment in exposure time.

this paper. Table 3 summarizes other functions and random variables that were discussed.

Table 4 presents plausible dose metrics that should be correlated to $B_j(t)$ or $B_n(t)$. They are the *specific cytoplasmic target surface area burden* $SURF_j(t)$ and the *specific nuclear surface area burden* $SURF_n(t)$, respectively; also the *specific cytoplasmic target mass burden* $MASS_j(t)$ and the *specific nuclear mass burden* $MASS_n(t)$, respectively. The expectation values for $SURF_j(t)$ (given by $W_j(t)$) and $MASS_j(t)$ (given by $Y_j(t)$) should be correlated with $M_j(t)$.The expectation values for $SURF_n(t)$ (given by $W_n(t)$) and $MASS_n(t)$ (given by $Y_n(t)$) should be correlated with $M_n(t)$.

The deterministic variables $W_j(t)$ and $W_n(t)$ are formally called *surface area burdens*. The deterministic variable $Y_j(t)$ and $Y_n(t)$ are formally called *mass burdens*. The metrics can be represented by respective covariate vectors $\mathbf{W}(t) = (W_j(t), W_n(t))$ and $\mathbf{Y}(t) = (Y_j(t), Y_n(t))$, which can be used in dose-response modeling.

It should be clear from the above that developing the capability for conducting a reliable risk assessment related to realistic MENAP expo-

TABLE 3. Variables and functions related to application of the STM Model to MENAP

Variable or Function	Explanation
N_j	Random number of cytoplasmic target particles to be exceeded to trigger autophagic-mode death
N_n	Random number of nuclear particles to be exceeded to trigger apoptotic-mode death
$\Phi_j(N_j)$	Distribution function for N_j
$\Phi_n(N_n)$	Distribution function for N_n
V_j	Average cytoplasmic target volume
V_n	Average nuclear volume
$C_{\max}\{V_j\}$	Maximum value for $M_j(t)$
$C_{\max}\{V_n\}$	Maximum value for $M_n(t)$
μ_j^*	Expectation value for N_j
μ_n^*	Expectation value for N_n
μ_j	Value for μ_j^* when N_j has a Poisson distribution.
μ_n	Value for μ_n^* when N_n has a Poisson distribution.
RP	MENAP relative potency
$T_{1/2}$	Halftime for cells being MENAP free

TABLE 4. Other dose metrics for MENAP that should be correlated with $B_j(t)$ or $B_n(t)$

Metric Formal Name[a]	Notation	Comment
Specific cytoplasmic target (e.g., mitochondria) surface area burden[b]	$SURF_j(t)$	Total surface area (added over the different particles in the cytoplasmic target); should be correlated with $B_j(t)$
Specific nuclear surface area burden[c]	$SURF_n(t)$	Total surface area (added over the different particles in the nucleus); should be correlated with $B_n(t)$
Specific cytoplasmic target (e.g., mitochondria) mass burden[b]	$MASS_j(t)$	Total mass load (added over the different particles in the cytoplasmic target); should be correlated with $B_j(t)$
Specific nuclear mass burden[c]	$MASS_n(t)$	Total mass load (added over the different particles in the nucleus); should be correlated with $B_n(t)$

[a]These formal names are introduced in this paper.
[b]The expectation value for this dose metric should be correlated with $M_j(t)$.
[c]The expectation value for this dose metric should be correlated with $M_n(t)$.

sure scenarios will require a multidisciplinary research team. Team members will need to provide expertise in the following areas:

- Expertise in obtaining and analyzing time-dependent images of MENAP in live cells.
- Expertise in quantitatively characterizing the distributions of $B_j(t)$ and $B_n(t)$ over the target cell population (*in vitro* and *in vivo*).

- Expertise in developing reliable particokinetic models for MENAP transport (*in vivo*), biodistribution (macroscopic), uptake by critical target cells and intracellular transport to the nucleus.
- Expertise in carrying out focused *in vitro* studies of MENAP-induced molecular and cellular effects that contribute to MENAP induced health effects: *MENAP RP for different particle characteristics and for different biological effects in vitro (e.g., DNA damage, mitochondria dysfunction, cytotoxicity, mutation induction, neoplastic transformation, etc.) are expected to be an important predictor of RP for specific health effects. For example, RP for neoplastic transformation is expected to be predictive of RP for cancer induction by MENAP.*
- Expertise in carrying out focused studies using animal models of MENAP induced health effects (e.g., nervous system dysfunction, pulmonary fibrosis, heart disease, cancer).
- Expertise in developing dose-response models (based on reliable dose metrics) for molecular, cellular, and systemic effects of exposure to MENAP: *The expertise should include the capability of integrating results from molecular, cellular, and animal studies of MENAP toxicity.*
- Expertise in computer code system development and implementation: *The expertise should include the ability to develop and link a dosimetric module that allows for different exposure scenarios to modules for specific health effects (e.g., cancer, cardiovascular disease) of MENAP. The dosimetric module should incorporate different sub-modules for implementing particokinetic and other models developed by other experts including models for environmental or workplace transport of MENAP to the human receptors, for uptake into the body, for systemic transport in the body, for uptake by critical target cells and transport to cell organelles. The health effects modules should incorporate dose-response models developed by other experts. For formal risk assessments for different exposures scenarios and target populations, a single flexible global computer code would be ideal.*

It can be seen from the above that establishing a capability to carry out reliable health risk assessment related to exposure of humans to MENAP is a major undertaking. If not properly planned and carried out, substantial financial and other resources could be wasted. It is important that modelers/theoreticians and experimentalist work together in planning and carrying out MENAP toxicology research. The modeling/theoretical work can help guide the experimental studies and the experimental work can in turn provide valuable information for model testing and refinement. This research implementation framework has been used quite successfully for many years in the physical sciences.

The development of the dose and dose rate metrics presented here was greatly facilitated by previous microdosimetric research related to exposure to ionizing radiation. Table 5 summarizes the correspondence between microdosimetric and related metrics introduce in this paper for

TABLE 5. Correspondence between MENAP and radiation microdose and macrodose concepts

	TYPE OF TOXICANT	
	MENAP	Radiation
Microdose Metrics	Specific cytoplasmic target or nuclear burden: $B_j(t)$ or $B_n(t)$	Specific energy z (dose to small tissue mass [e.g., single cell nucleus])
Microdose Expectation Value	Cytoplasmic target or nuclear burden: $M_j(t)$ or $M_n(t)$	Absorbed dose D (dose to target tissue)
Modifiers of Potency	Possible modifiers: stability, porosity, density, shape, surface area, surface charge density, surface reactivity, hydrophobicity, interactions with biomolecules (e.g., corona), biological target hit rate	Lineal energy (microscopic metric); linear-energy-transfer, absorbed dose rate

characterizing MENAP cytotoxicity and those used for characterizing radiation cytotoxicity. The radiation-related microdose metrics allow predicting the expected relative potency of different types of radiation for inducing stochastic effects such as mutations (Varma *et al.* 1985). The relative potency for different radiation is formally called relative biological effectiveness. Possibly, this approach to predicting relative potency based on first principals could also be realized for MENAP; however, *in order to achieve this goal, it will be necessary to generate experimental databases that allow identification of key factors that influence MENAP potency.* Possible influencing factors are also listed in Table 5 and include stability, porosity, density, shape, surface area, reactivity, hydrophobicity, and interaction with biomolecules in surrounding media. New research is needed to clarify the relative importance of these factors.

ACKNOWLEDGEMENTS

This research was supported by the Office of Science (BER), U.S. Department of Energy, Grant No. DE-FG02-09ER64783. I am grateful the journal reviewers and to Dr. Jean Clare (Jinkle) Seagrave for their helpful suggestions related to the manuscript and to Wendy Piper and Vincent Ramirez for graphics support.

REFERENCES

AshaRani PV, Hande MP, and Valiyaveettil S. 2009. Anti-proliferative activity of silver nanoparticles. BMC Cell Biology 10: Electronic version available at http://www.biomedcentral.com/1471-2121/10/65.

Bursch W, Hochegger K, Torok L, Barian B, Sllinger A, Hermann RS. 2000. Autophagic and apoptotic types of programmed cell death exhibit different fates of cytoskeletal filaments. J Cell Sci 113:1189-1198

Gamerman D. 1997. *Markov Chain Monte Carlo, Stochastic Simulation for Bayesian Inference*, Chapman & Hall, London

Gelman A, Carlin JB, Stern HS, and Rubin DB. 1995. *Bayesian Data Analysis*, Chapman and Hall, London

Decisioneering. 2001. *Crystal Ball Users Manual*, Decisioneering, Inc., Denver, Colorado.

Donaldson K, Stone V, Tran CL, Kreyling W, and Borm PJ. 2004. Nanotoxicology. Occup Environ Med 61:727-728

Hardman RA. 2006. Toxicology review of quantum dots: Toxicity depends on physio-chemical and environmental factors. Environ Health Perspect 114(2):165-172

Lunn DJ, Thomas A, Best N, and Spiegelhalter D. 2000. WinBUGS–a Bayesian modeling framework: concepts, structure, and extensibility. Statistics and Computing 10:325-337

Moghimi SJ, Hunter AC, and Murray JC. 2005. Nanomedicine: current status and future prospects. FASEB J 19:311-330

Oberdörster G, Oberdörster E, and Oberdörster J. 2005. Nanotoxicology: an emerging discipline evolving from studies of ultrafine particles. Environ Health Perspect 112(7):823-839

Powell MC, Kanarek MS. 2006a. Nanomaterial health effects–Part 1: Background and current knowledge. WMJ 105(2):16-20

Powell MC and Kanarek MS. 2006b. Nanomaterial health effects–part 2: uncertainties and recommendations for the future. WMJ 103(3):18-23

Prabhu BM, Ali SF, Murdock RC, Hussain SM, and Srivatsin M. 2009. Copper nanoparticles exert size and concentration dependent toxicity on somatosensory neurons of rat. Nanotoxicology 3(4):1-10

Rabiner LR. 1989. A tutorial on hidden Markov models and selected applications in speech recognition. Proceedings of the IEEE 77(2):257-286

Redpath JL, Liang D, Taylor TH, James C, Christie E, and Elmore E. 2001. The shape of the dose-response curve for radiation-induced neoplastic transformation in vitro: evidence for an adaptive response against neoplastic transformation at low doses of low-LET radiation. Radiat Res 156:700-707

Roco MC. 2005. Societal implications of nanoscience and nanotechnology: maximizing human benefit. J nanopart Res 7:129-143

Scott, B. R. 2005. Stochastic thresholds: A novel explanation of nonlinear dose-response relationships. Dose-Response 3: 547-567

Scott BR., Belinsky SA, Leng S, Lin Y, Wilder JA, and Damiani LA. 2009. Radiation-Stimulated Epigenetic Reprogramming of Adaptive-Response Genes in the Lung: An Evolutionary Gift for Mounting Adaptive Protection against Lung Cancer. Dose Response 7(2): 104-131

Varma MN, Bond VP, Matthews G. 1985. Hit-size effectiveness theory applied to high doses of low LET radiation for pink mutations in tradescantia. Radiat Prot Dosim 13(1-4):307-309